MATHEMATICAL MODELLING OF HYSTERESIS LOOPS FOR REINFORCED CONCRETE COLUMNS

by

Shinsuke NAKATA[I], Terry SPROUL[II], Joseph PENZIEN[III]

SUMMARY

The objective of this research is to estimate lateral force-deflection curves for reinforced concrete columns subjected to cyclic transverse loads and constant axial loads. These curves are determined in relation to the column parameters such as shear-span ratio, longitudinal and horizontal reinforcement, and axial force.

The test data of columns for this research were obtained from 104 specimens.

Summary equations are developed by statistical methods. The hysteresis loops generated from the empirical equations are in good agreement with the test data.

1. INTRODUCTION

Up to now empirical expressions for only a few types of strength and the stiffness at bending yield for unidirectional loading have been developed as mathematical models based on member parameters.[1-17]

Recently, digital test data became available for lateral load deflection relationships for short columns. These had been developed systematically in Japan.[18] This digital information is used in the following to predict the shape of hysteresis loops by statistical procedures.

2. TEST DATA

Many structures with short columns have suffered serious damage in recent earthquakes in many parts of the world. In 1972 a large five-year test project was started in Japan to establish new earthquake resistant design methods for such structures. In that project, test data were gathered from about 300 columns subjected to cyclic transverse loads under constant axial loads.

Short columns have been adopted in this program with shear span ratios of 1.0, 1.5, 2.0, 2.5 and 3.0 taken as standard. In this program, the design of shear reinforcement ratio, P_w, is based on Arakawa's[19] formula in which the mean shear stress at flexural yield strength is used. The shape of the hoops is mainly square with 135° hooks.

Fig.1 shows the typical specimen details for all the tests, the scale of the cross section, and the covering and anchoring of the main reinforcement. The test specimen is subjected to antisymmetric moment and constant axial load without the top and bottom of the column rotating. Fig.2 shows the system of cyclic loading controlled by the deflection of the top relative to the bottom of the column. Each amplitude is based on the deflection, δ_y, at flexural yield, which is obtained from a loading test for each specimen. Fig.3 shows crack patterns developing during the test procedure. The typical failure modes that were observed are as follows:

I Chief Engineer of Buildg. Res. Inst., Min. of Construction, JAPAN.
II Research Assistant of Univ. of California, U.S.A.
III Professor of Univ. of California, U.S.A.

1) Shear failure prior to flexural yielding
2) Bond failure prior to flexural yielding
3) Shear failure after flexural yielding
4) Bond failure after flexural yielding
5) Steel bucking after flexural yielding
6) Compressive failure of concrete after flexural yielding.

The test specimens were mainly selected from the failure category 3), 4), and 5). The number of specimens suitable for the statistical procedure was 104. The shear span ratio, a/d, was either 1.0, 1.5, 2.0, 2.5 or 3.0, and the majority of the specimens had a/d = 2.0.

The columns were subjected to constant axial stress, P/bd, (ranging from -21 kg/cm^2 to 70 kg/cm^2) during the loading. The compressive strength fc' of the concrete used in these specimens ranges from 153 kg/cm^2 to 453 kg/cm^2. The longitudinal tensile reinforcement ratio, P_t, is the same as the compressive reinforcement ratio in the cross-section of each specimen, and their values are mainly 0.4 percent, 0.6 percent, and 0.95 percent. The value of the shear reinforcement ratio is distributed between 0.09 percent and 2.44 percent. None of the specimens failed in shear before flexural yield.

From the enlarged graphs of the hysteresis loops, the first, the third, and tenth cycles at 1δy, 2δy, 3δy and 4δy were reduced to digitized form.

The lateral force-deflection data of each hysteresis loop (more than 40 points in one loop) were replaced by slopes, deflections, and shear forces at special points of the loop for use in the statistical procedure.

The reduced data set consists of 20 points for each specimen in each cycle as shown in Fig.4. Points 1 to 10 are in the region of positive loading, and points 11 to 20 are in the region of negative loading. Points 1 to 5 and 11 to 15 are the slopes of the curve (in ton/mm). Deflections 6 and 16 are the maximun deflections, and deflections 9 and 19 are the remaining deflections when the load is zero. Shear forces 8 and 18 are the loads when the loop crosses the load axis; shear forces 7 and 17 are the loads at maximum deflection.

Point 10 is the area of the loop on the positive load side, and point 20 is the corresponding area on the negative side. After checking data at loading and unloading in each of the regions defined above, the set 21 to 30 was computed as shown in Fig.4. Points 21 to 25 are average dimensionless stiffness ratios based on the "peak to peak" stiffness, 27/26. In this way about eighty digital figures (40 points) in one hysteresis loop were reduced to ten digital data.

3. EMPIRICAL EQUATIONS OF HYSTERESIS LOOPS

3.1 Outline of Estimated Hysteresis Loops In this section, the authors are searching for empirical equations D1, D2, D3, ... D9 which are developed from the test data 21, 22, 23, ... 29 by statistical processes.[20] The skeleton curve is defined as shown in Fig.5. The shear force Q_y, the deflection δy (D6) at flexural yield and the envelope curve after flexural yielding are obtained experimentally as estimated equations. The curve from the origin to the yield point is assumed to be parabolic. This curve opens downwards and the maximum value is Qy. As a second step, a hysteresis loop is defined in terms of six elements as shown in Fig.6. The six empirical equations are D1, D2, D3, D5, D8, and D9, and cubic equations based on the test data are used between each adjacent pair of elements.

3.2 Skeleton Curve The calculated shear force, Q_{yc}, at flexural yielding,

which is based on plastic reinforced concrete theory, does not always agree with the test value, Q_{yt}, especially for short columns. Fig.7 shows the average values of Q_{yt}/Q_{yc} for each combination of parameters. In the top diagram, the test specimens are separated into domains according to their shear span ratio 1.0 and 1.5; 2.0; 2.5 and 3.0. In the second diagram the three groups are each divided into two domains determined by shear reinforcement ratio < 1.2 percent or ≥ 1.2 percent. Similarly, the third diagram is the distribution of longitudinal reinforcement, and the fourth one is the distribution of axial stress divided by concrete strength.

Fig.8.a shows the comparison between the experimental values Q_{yt} and calculated values Q_{yc} used so far. In the next curve, Fig.8.b, the calculated value has been corrected to αQ_{yc}, where α is obtained by assuming a linear relation among the four test parameters and the method of least squares is applied to obtain the coefficients.

$$\alpha = 1.418 - 0.105\ a/d - 12.49\ Pt - 7.37\ P_w - 0.464\ P/bdf'_c.$$

Equation 3.1, represented as D7, is obtained from an analysis of the data distributions in Fig.7.

$$D7(\text{yield}) = 0.801 + (0.623 - 29.07\ P_t - 5.623\ P_w - 1.11\ P/bdf'_c)/(a/d) \quad \ldots\ldots (3.1)$$

Then the ordinate of Fig.8.c has been corrected to $D7(\text{yield}) \cdot Q_{yc}$. A comparison of the three diagrams, Fig.8.a, b and c indicates that Fig.8.c gives the best estimate for shear force at flexural yielding. Using the graphs of the average rotational angle, δ_y/h, at flexural yielding for each parameter combination, where h is the clear span of the column, we could get following equation.

$$D6 = \delta_y/h = 0.005 - 0.00124\ a/d + 0.63\ P_t - 0.056\ P_w. \qquad (3.2)$$

Fig.9.a shows the comparison of the experimental results with Eq. (3.2). Although the accuracy is not satisfactory in this diagram, the error is less than in Fig.9.b in which a comparison is made between the test results and an empirical equation developed by Sugano using other test data. Hence Eq. (3.2) is adopted to estimate δ_y/h.

The following estimated equation, D7, of the envelope curve and force reduction ratio by cyclic loads are obtained by the same method of least squares:

$$D7(\text{envelope}) = 1.0577 + (a/d - 3.0)(3.777\ P_t - 0.0221\ P/bdf'_c)\ \text{amp} \quad \ldots\ldots (3.3)$$

where amp is the dimensionless amplitude, δ/δ_y; δ_y is calculated for each specimen from Eq. 3.2.

$$D7(\text{cycle}) = 1.046 - 0.00554\ a/d - 0.0345\ \text{cycle}/(a/d) + (P_t - 0.004)(-0.013 + 2.569\ P/bdf'_c - 5.98\ \text{amp}) \qquad (3.4)$$

These two equations demonstrate the dependence of some parameters in D7(cycle) on other parameters.

If an arbitary shear force is needed, it is obtained as follows:

$$Q = D7(\text{amp}) \cdot D7(\text{cycle}) \cdot Q_{yc}$$

3.3 Hysteresis Loop Using the test data, the element D1 to D9 (Fig.6) used to characterize the shape of the hysteresis loop, are now defined. A hysteresis loop is defined by pairs of equations. Each pair consists of one equation for amplitude, and the other for cyclic loading with fixed amplitude.

Applying the same techniques used in Section 3.2, these estimated equations D1, D2, ... D9 are summarized in Table 1, which also shows the trend of the parameters with the elements. In each case a pair of equations is used as follows: Using D1 as an example, the first cycle at a given amplitude would be described by D1(amp). All subsequent cycles at that deflection would be described by D1(amp).D1(cycle).

4. ESTIMATED HYSTERESIS LOOPS

The hysteresis loops are drawn using cubic or parablic equations. First, as shown in Fig.5 the initial curve 0A is a parabolic equation whose maximum value is at δ_y. In the cyclic hysteresis loop, as shown in Fig.6, the half cycle consists of three sections --- RANGE 1, RENGE 2 and RANGE 3; the first two are cubic polynomials and the third is a parabola. The boundary conditions for these have already been calculated in Section 3. Some examples of estimated hysteresis loops (CASE 1, CASE 2,...CASE 4) are shown in Fig.10. These are compared with the test results. The graphs show that the "estimated model" agrees reasonably well with the test results.

In these figures, the three loops correspond to the first, third and tenth cycles of each amplitude. CASE 1: small shear span ratio($a/d = 1.0$), small shear reinforcement ($P_w = 0.21\%$); the shape of hysteresis loops obtained from test data is that of the hard spring type even for the initial amplitude. For such a combination of parameters, there is a rapid reduction of shear force. The predicted hysteresis loops demonstrate these results reasonaly well. CASES 2 and 3: $a/d = 1.5$. The different longitudinal reinforcements of these two cases changes the shapes of the loops. The estimated hysteresis loops also demonstrate this delicate difference. CASE 4: $a/d = 3.0$. It shows that the estimated hysteresis loops agree reasonably well with test data which shape is stable.

5. CONCLUSIONS AND RECOMMENDATIONS

The proposed method of predicting hysteresis loops for reinforced concrete columns involves using test data statistically. The estimated hysteresis loops are obtained by a series of simple, statistical procedures and agree reasonably well with the test data for the following:

1) Change in shear force for a given amplitude and number of cyclic loads.
2) Shape of the hysteresis loops.
3) Shear force and deflection at bending yield for short columns.

It is important to note, however, that this evaluation is based upon test data for columns which never failed in shear or bond before flexural failure. There are no test data for loops in these cases.

For a complete estimation of the load deflection relationship, we recommend that cyclic loading tests of longer columns ($a/d = 3.5$, 4.0 and 5.0) should be developed systematically.

It should be noted that the estimated equations presented herein are developed only for this particular set of test data. Further work is needed in order that these equations may be applied to the more general case of nonrepetitive cyclic loading.

REFERENCES

1. Ramberg, W., and Osgood, W.R., "Description of Stress-Strain Curves by Three Parameters," NACA TN 902, July 1943.
2. Jennings, P.C., "Response of Yielding Structures to Statistically Generated Ground Motion," III W.C.E.E., New Zealand, 1965.
3. Iwan, W.D., "The Distributed-Element Concept of Hysteretic Modeling and its Application to Transient Response Problems," IV W.C.E.E., Santiago, Chile, 1969.
4. Clough, R.W., and Johnston, S.B., "Effect of Stiffness Degradation on Earthquake Ductility Requirements," Proceedings of Japan Earthquake Engineering Symposium, Tokyo, October 1966.
5. Liu, Shih-Chi, "Earthquake Response Statistics of Nonlinear Structures," ASCE Proceedings, Journal of Engineering Mechanics Division, Vol. 95, EM2, April 1969.
6. Goel, S.C., "Inelastic Behavior of Multistory Building Frames Subjected to Earthquake Motion," University of Michigan, 1967. (Thesis).
7. Shiga, T., and Ogawa, J., "The Experimental Study on the Dynamic Behavior of Reinforced Concrete Frames," Proceedings IV World Conference on Earthquake Engineering, B-2, pp. 165-176, Santiago, Chile, 1969.
8. Takeda, T., Sozen, M.A., and Nielsen, N.N., "Reinforced Concrete Response to Simulated Earthquakes," Proceedings ASCE Vol. 96 (ST12), Journal of the Structural Div., December 1970.
9. Kent, D.C., "Inelastic Behavior of Reinforced Concrete Members with Cyclic Loading," Ph.D. Thesis, Univ. of Canterbury, Christchurch, New Zealand, 1969.
10. Otani, S., and Sozen, M.A., "Behavior of Multistory Reinforced Concrete Frames During Earthquakes," Civil Engineering Studies, Structural Research Series No. 392, Univ. of Illinois, Urbana, November 1972.
11. Bertero, V.V., "Effects of Generalized Excitations on the Nonlinear Behavior of Reinforced Concrete Structures," Proceedings of the International Conference on Planning and Design of Tall Buildings, IABSE-ASCE, Vol. III, pp. 431-453, Lehigh Univ., Bethlehem, Pennsylvania, August 1972.
12. Bertero, V.V., Bresler, B., and Liao, H.M., "Stiffness Degradation of Reinforced Concrete Members Subjected to Cyclic Flexural Moments," Report No. EERC 69-12, Univ. of California, Berkeley, December 1969.
13. Celebi, M., and Penzien, J., "Experimental Investigation into the Seismic Behavior of Critical Regions of Reinforced Concrete Components as Influenced by Moment and Shear," Report No. EERC 73-4, Univ. of California, Berkeley, January 1973.
14. Ataley, M.B., and Penzien, J., "The Seismic Behavior of Critical Regions of Reinforced Concrete Components as Influenced by Moment, Shear and Axial Force," Report No. EERC 75-19, Univ. of California, Berkeley, December 1975.
15. Wight, J.K., and Sozen, M.A., "Shear Strength Decay in Reinforced Concrete Columns Subjected to Large Deflection Reversals," Civil Engineering Studies, Structural Research Series No. 403, Univ. of Illinois, Urbana, August 1973.
16. Sugano, S., and Koreishi, I., "An Empirical Evaluation of Inelastic Behavior of Structural Elements in Reinforced Concrete Frames Subjected to Lateral Forces," Proceedings of the Fifth World Conference on Earthquake Engineering, Vol. I, Rome, 1974.
17. Hirosawa, M., "Synthetic Research on Preventing Reinforced Concrete Columns from Total Collapse (in Japanese)," Building Research Institute, Japan, BRI Research Paper, 1972.
18. Building Research Institute, Japan, Committee on Reinforced Concrete Structures in Building, "The Experimental Study on the Behavior of the Reinforced Concrete Columns under Cyclic Loading," (AR-1 Series, AR-2 Series, LM-2 Series, AF Series, WS Series, LS Series, Pilot Series, FC Series, DCW-1 Series, DCW-2 Series, SE Series), 1972-1976.
19. The 1971 Architectural Inst. of Japan Standard for Structural Design of Reinforced Concrete Construction.
20. Brownlee, K.A., "Statistical Theory and Methodology in Science and Engineering," John Wiley & Sons, Inc., 1965.

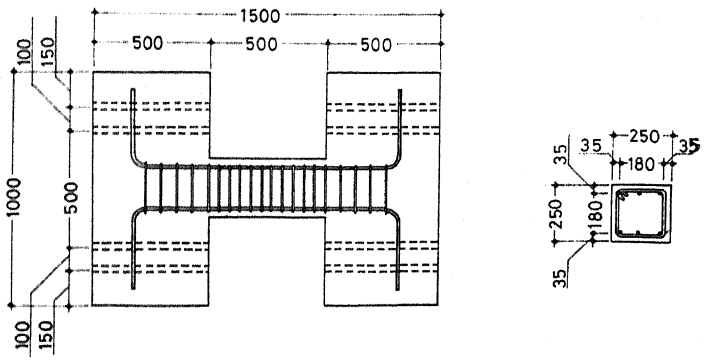

Fig.1 Specimen Details

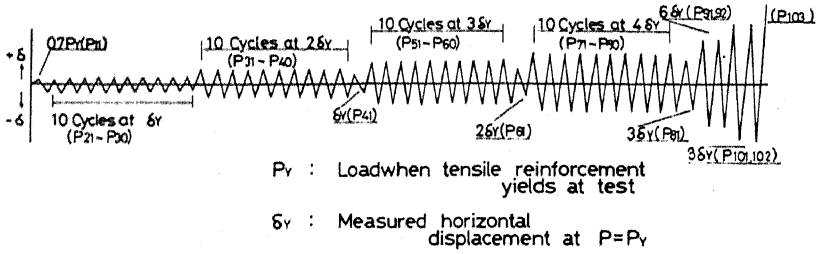

P_y : Load when tensile reinforcement yields at test

δ_y : Measured horizontal displacement at $P=P_y$

Fig.2 Cyclic Loading System

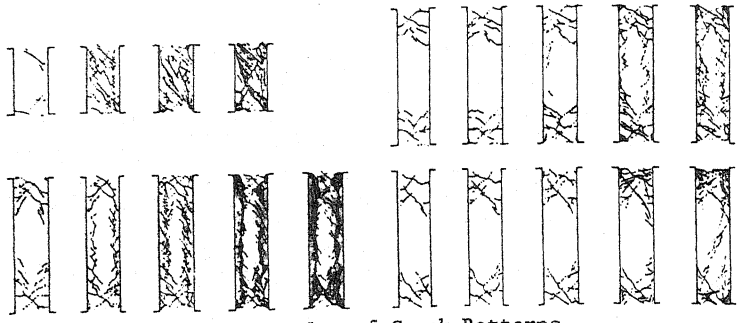

Fig. 3 Examples of Crack Patterns

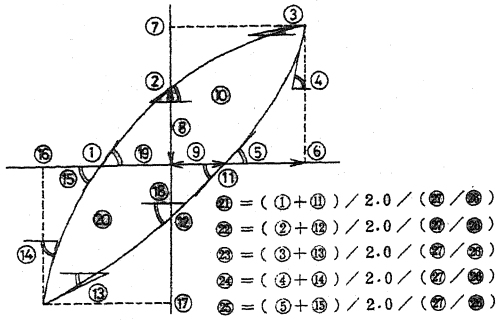

㉑ = (① + ⑪) / 2.0 / (㉗ / ㉘)
㉒ = (② + ⑫) / 2.0 / (㉗ / ㉘)
㉓ = (③ + ⑬) / 2.0 / (㉗ / ㉘)
㉔ = (④ + ⑭) / 2.0 / (㉗ / ㉘)
㉕ = (⑤ + ⑮) / 2.0 / (㉗ / ㉘)
㉖ = (⑥ + ⑯)
㉗ = (⑦ + ⑰)
㉘ = (⑧ + ⑱) / ㉗
㉙ = (⑨ + ⑲) / ㉘
㉚ = (⑩ + ⑳)

Fig.4 Data Reduction

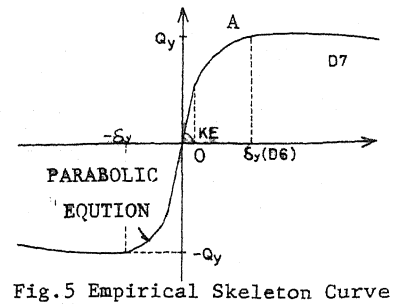

Fig.5 Empirical Skeleton Curve

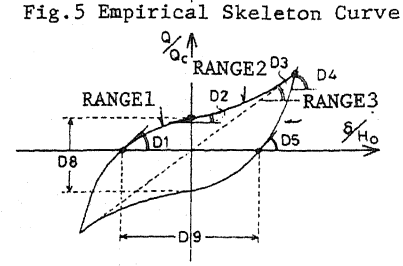

Fig.6 Empirical Hysteresis Loop

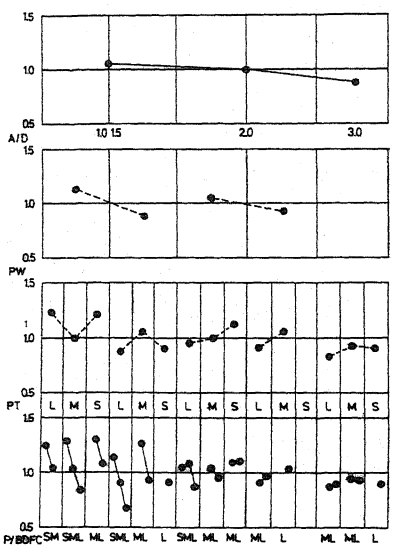

Fig.7 Average Value in Each Parameter Domain

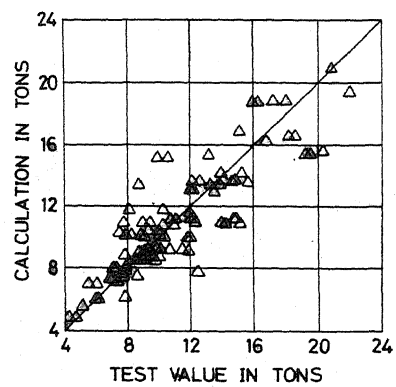

Fig.8 a Comparison Between Calc. Value & Test Value of Q_y

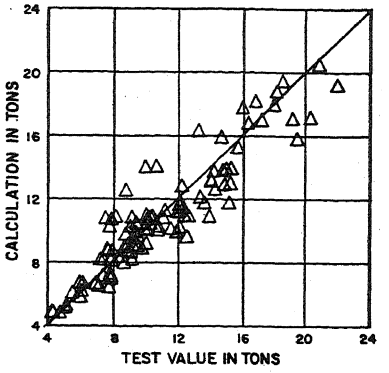

Fig.8 b Comparison Between Calc. Value αQ_y & test Value

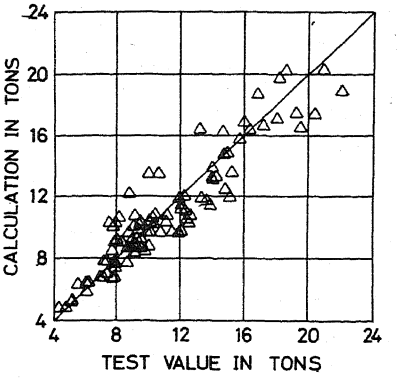

Fig. 8 c Comparison Between Calc. Value $D7 \cdot Q_y$ & Test Value

Table 1 Estimated Equations

	inclination of effective Parameter				remarks
D1	A/D	UP	D1(AMP)	UP	
	Pw	"		DOWN	restained by A/D
	Pt	"		"	
	P/BDFc	"		UP	"
	AMP	"		DOWN	"
	D1(AMP)=1.354+(3.5-A/D)(0.542-5.126Pw-49.9Pt+0.51P/BDFc-0.153AMP)				
	AMP	UP	D1(CYCLE)	UP	restrained by Pt
	CYCLE	"		"	logarithm
	D1(CYCLE)=0.067+8.93AMP(Pt+0.005)				
D2	Pt	UP	D2(AMP)	DOWN	restrained by A/D
	Pw	"		"	"
	AMP	"		"	"
	D2(AMP)=1.481+(A/D-3.0)(41.08Pt-10.09Pw+0.07AMP)				
	CYCLE	UP	D2(CYCLE)	DOWN	
	AMP	"		UP	
	D2(CYCLE)=0.844-0.031CYCLE+0.031AMP				
D3	CYCLE	UP	D3(AMP,CYCLE)	UP	logarithm
	Pt	"		"	restrained by A/D
	P/BDFc	"		DOWN	"
	AMP	"		UP	"
	D3(AMP,CYCLE)=-0.381+(4-A/D)(33.347Pt-0.026AMP)				
D5	A/D	UP	D5(AMP)	UP	
	Pt	"		DOWN	restrained by A/D
	AMP	"		UP	"
	D5(AMP)=1.054+(A/D-3)(0.024+12.128Pt-0.039AMP)				
	CYCLE	UP	D5(CYCLE)	UP	restrained by A/D
	AMP	"		"	"
	D5(CYCLE)=0.972+(3.5-A/D)(-0.114+0.014CYCLE+0.05AMP)				
D8	Pt	UP	D8(AMP)	DOWN	restrained by A/D
	AMP	"		CHANGE	"
	D8(AMP)=0.239+5.88(A/D-3)Pt+0.0144AMP(A/D-2.3)				
	CYCLE	UP	D8(CYCLE)	DOWN	
	AMP	"		UP	restrained by Pt
	D8(CYCLE)=0.842+0.0004SCYCLE+13.559(Pt-0.002)AMP				
D9	Pt	UP	D9(AMP)	UP	restrained by AMP
	A/D	"		"	"
	D9(AMP)=0.1656+(6.78(Pt-0.002)+0.0184A/D)AMP				
	CYCLE	UP	D9(CYCLE)	DOWN	
	AMP	"		UP	

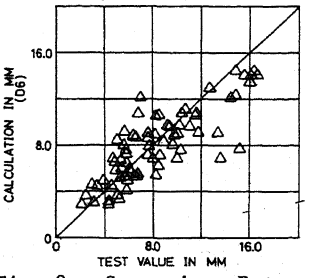

Fig. 9 a Comparison Between Calc. Value D6 & Test Value δ_y

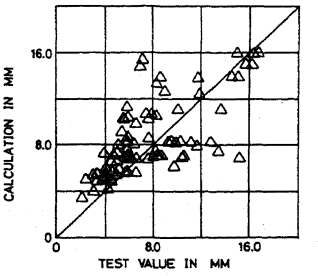

Fig. 9 b Comparison Between Sugano's Calc. Value & Test Value

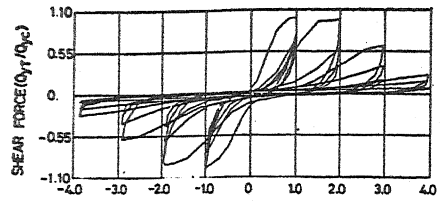

CASE 1

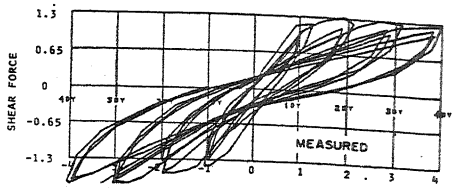

CASE 2

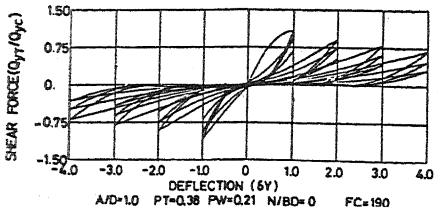

A/D=1.0 PT=0.38 PW=0.21 N/BD= 0 FC=190

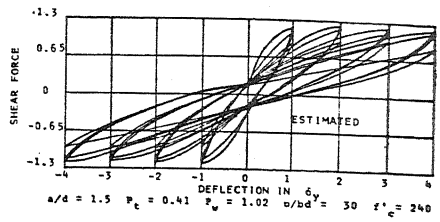

a/d = 1.5 P_t = 0.41 P_w = 1.02 n/bd = 30 f'_c = 240

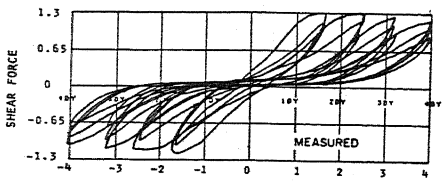

CASE 3

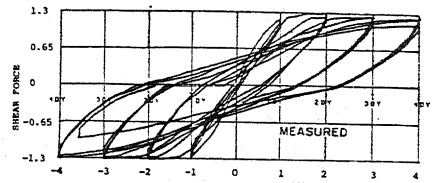

CASE 4

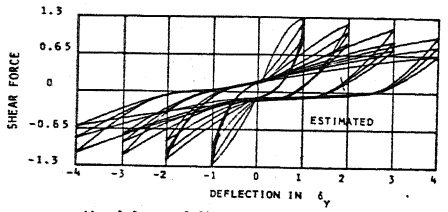

a/d = 1.5 P_t = 1.24 P_w = 2.12 P/bd = 30 f'_c = 207

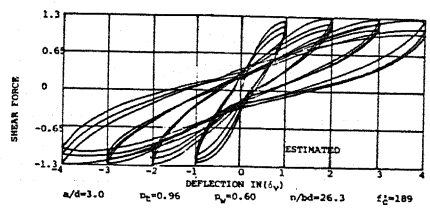

a/d=3.0 P_t=0.96 P_w=0.60 n/bd=26.3 f'_c=189

Fig. 10 Empirical Hysteresis Loops